PHYSICAL REVIEW B VOLUME 52, NUMBER 6 1 AUGUST 1995-II

Onset of superconductivity in the antiferromagnetically ordered state of single-crystal $DyNi_2B_2C$

B. K. Cho, P. C. Canfield, and D. C. Johnston
Ames Laboratory and Department of Physics and Astronomy, Iowa State University, Ames, Iowa 50011

(Received 15 March 1995)

Temperature-dependent static magnetization, ac magnetic susceptibility, and electrical-resistivity measurements of single-crystal $DyNi_2B_2C$ reveal bulk superconductivity below $T_c=(6.2\pm0.1)$ K. This T_c is well below the Néel temperature $T_N=10.3$ K. $DyNi_2B_2C$ is the first RNi_2B_2C compound with $T_c<T_N$. The upper critical magnetic field $H_{c2}(T)$ increases approximately linearly from zero at 6.2 K to ~5 kG at 2 K.

The interplay between superconductivity and local-moment magnetism has been vigorously studied since the late 1950s.[1] In the 1970s the discovery of two families of magnetic superconductors, $RMo_6(S,Se)_8$ and RRh_4B_4 (R = rare earth), led to a detailed study of the interaction between the magnetic sublattice and the superconducting electrons.[1] Recently the RNi_2B_2C family of magnetic superconductors was discovered.[2] For R = Lu, Y, Tm, Er, and Ho the superconducting transition temperatures for single-crystal samples are $T_c=16.0$, 15.0, 10.8, 10.5, and 8.5 K, respectively.[3–7] Superconductivity coexists with antiferromagnetic (AF) order for R = Tm, Er, and Ho for temperatures below the Néel temperatures $T_N=1.5$, 5.85, and 6.0 K, respectively.[4–7,9,10] Similar values of T_c and T_N have been found for polycrystalline samples.[2,8] In virtually all known magnetic superconductors,[11] when there is a coexistence of AF ordering and superconductivity, $T_c>T_N$. The only local-moment systems that have $T_c<T_N$ are solid solutions such as the $R(Ir_xRh_{1-x})_4B_4$ system where $T_N=2.7$ K and $T_c=1.4$ K for R = Ho and $x=0.7$.[1,12] This reversal of T_c and T_N only occurs for $0.6<x<0.8$ in this alloy. Compounds exhibiting $T_c<T_N$ are expected to be rare since the stronger the conduction electron-local moment coupling (such as would be required for a higher T_N), the greater the anticipated suppression of T_c through magnetic pair breaking.[1] In this paper we report the discovery of superconductivity in single-crystal $DyNi_2B_2C$ below a $T_c=(6.2\pm0.1)$ K that is well below the $T_N=10.3$ K. This is the first such member of the RNi_2B_2C family with $T_c<T_N$.

Single crystals of $DyNi_2B_2C$ were grown from Ni_2B flux[3] using high-purity elements: B (99.9%), Ni (99.99%), C (99.99%), and Ames Lab Dy (99.99%). The crystals grow in the form of plates with the crystallographic c axis perpendicular to the largest plate surface. The static magnetization M was measured using a Quantum Design (SQUID) magnetometer and the ac susceptibility χ_{ac} was measured using a Lakeshore ac magnetometer. The single crystal used for the M and χ_{ac} measurements had approximate dimensions of $2.5\times2.5\times0.7$ mm^3. The four-lead electrical resistivity ρ_{ab} was measured on a platelike crystal with the current flowing in the basal ab plane using a Linear Research, LR 400, ac resistance bridge operating at 15.9 Hz.

Figure 1 shows the powder x-ray-diffraction pattern of a crushed single crystal of $DyNi_2B_2C$. The diffraction peaks index well to the tetragonal unit cell reported[2] for $DyNi_2B_2C$ with lattice parameters $a=3.534$ Å and $c=10.484$ Å. The only peak that is not indexed to $DyNi_2B_2C$ is the weak peak at $2\theta=45.85°$, attributed to the [211] peak of the Ni_2B flux.[13]

Figure 2 displays the temperature-dependent magnetic susceptibility $\chi(T)$ of $DyNi_2B_2C$ with a magnetic field $H=1$ kG applied parallel ($\mathbf{H}\|c$) and perpendicular ($\mathbf{H}\perp c$) to the c axis. Magnetic neutron diffraction measurements[14] indicate that the sharp feature at $T_N=10.3$ K in Fig. 2 should be attributed to the onset of AF order. The large anisotropy seen between $\mathbf{H}\|c$ and $\mathbf{H}\perp c$ at low T is a feature common to the RNi_2B_2C materials for R = Er, Ho, and Tb.[6,7,15] The inset to Fig. 2 shows $\chi^{-1}(T)$ for both directions of applied field as well as for the polycrystalline average of the $\chi_{\|c}$ and $\chi_{\perp c}$ data: $\chi_{poly}=\chi_{\|c}/3+2\chi_{\perp c}/3$. The $\chi_{poly}(T)$ data can be fitted by a Curie-Weiss law $\chi=C/(T-\theta)$ for $20<T<350$ K, giving an effective moment $\mu_{eff}=9.85\mu_B$ and $\theta=(1\pm2)$ K. This value of μ_{eff} is slightly lower than the theoretical value of $10.63\mu_B$ for the $J=15/2$ Hund's rule ground state of Dy^{3+}. The anisotropic $\chi(T)$ data can also be fitted by a Curie-Weiss form for $\mathbf{H}\|c$ for 230 K $<T<$375 K giving $\mu_{eff}=10.4\mu_B$ and $\theta=-82$ K and for $\mathbf{H}\perp c$ for 200 K$<T<$325 K giving $\mu_{eff}=9.8\mu_B$ and $\theta=25$ K.

Figure 3(a) shows $\rho_{ab}(T)$ of a $DyNi_2B_2C$ crystal. There is a sharp loss of scattering associated with the AF transition at

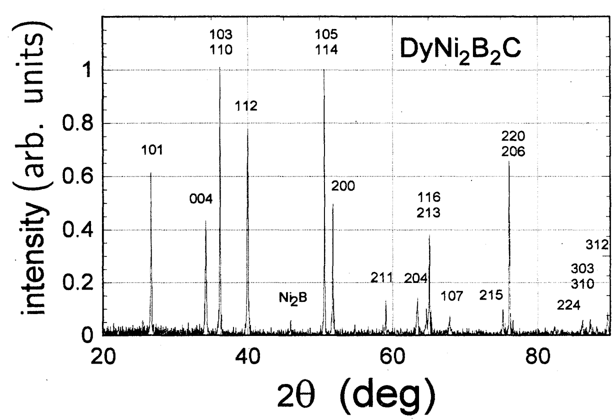

FIG. 1. Powder x-ray-diffraction pattern of a crushed $DyNi_2B_2C$ single crystal.

 © 1995 The American Physical Society

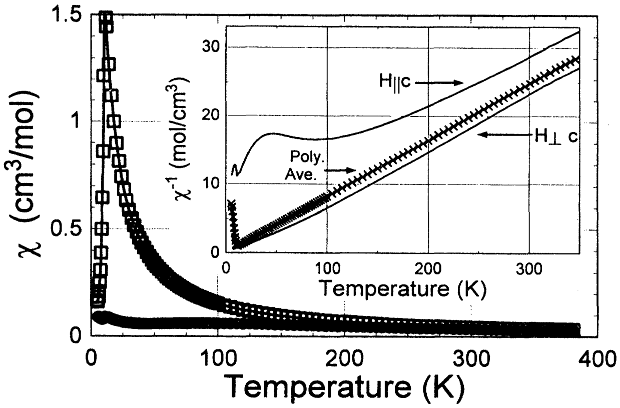

FIG. 2. Anisotropic magnetic susceptibility χ vs temperature T for $DyNi_2B_2C$, with $\mathbf{H}\perp c$ (squares) and $\mathbf{H}\| c$ (circles) and $H=1$ kG. Inset: Anisotropic (and polycrystalline average) χ^{-1} vs T.

$T_N = 10.3$ K, followed by a superconducting transition with an onset at 6.4 K and zero resistivity at 6.0 K. We find $\rho_{ab}(300\ \text{K}) = 55\ \mu\Omega$ cm. The residual resistivity ratio is $\rho_{ab}(300\ \text{K})/\rho_{ab}(7\ \text{K}) = 27$ indicating that the crystal has a high degree of perfection. Figure 3(b) shows $\rho_{ab}(H,T)$ for $2\ \text{K}<T<7\ \text{K}$ and $\mathbf{H}\perp c$. For these applied fields ($H \leqslant 5$ kG), T_N is only weakly field dependent, decreasing to $T_N = 10.0$ K for $H=5$ kG (not shown). As can be seen from Fig. 3(b), T_c is suppressed and the width of the superconducting transition is increased with increasing H.

Figure 4 shows the temperature-dependent upper critical magnetic field $H_{c2}(T)$ derived from the $\rho_{ab}(H,T)$ data in

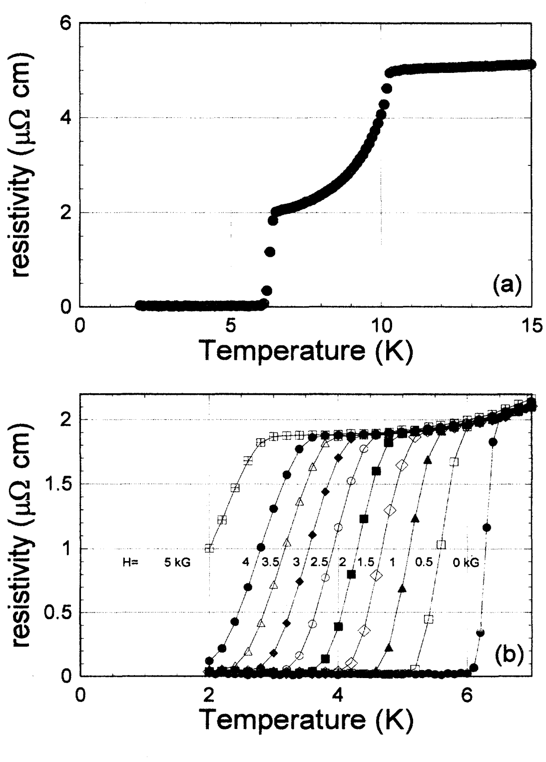

FIG. 3. Electrical resistivity of $DyNi_2B_2C$ in the ab plane vs temperature T: (a) $H=0$ and $T<15$ K and (b) $\mathbf{H}\perp c$ and $T<7$ K.

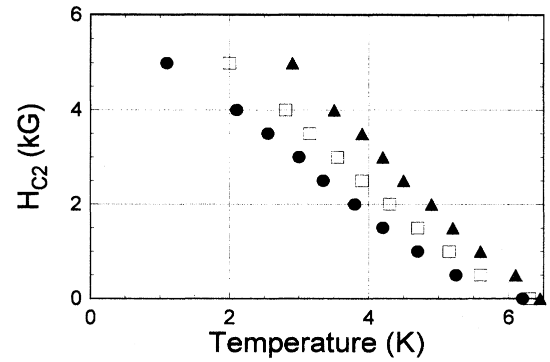

FIG. 4. Upper critical magnetic field H_{c2} vs temperature T for $DyNi_2B_2C$ with $\mathbf{H}\| c$. The circles, squares, and triangles show $H_{c2}(T)$ data determined from Fig. 3(b) by using the zero-resistivity, midpoint, and resistive onset, respectively, as the criterion for determining $T_c(H)$.

Fig. 3(b). $H_{c2}(T)$ increases nearly linearly with decreasing T from 10 G [just below $T_c(H=0)$] to ~ 5 kG near 2 K. No local minimum or other structure is seen in $H_{c2}(T)$, which is consistent with $T_c < T_N$. This is in contrast to the local extrema in $H_{c2}(T)$ seen for $TmNi_2B_2C$,[5,8] $ErNi_2B_2C$,[6,8] and $HoNi_2B_2C$.[7,8] The value of $\|dH_{c2}/dT\|_{T_c} = (1.2 \pm 0.2)$ kG/K is less than the values of (2.8 ± 0.2) and (2.6 ± 0.2) kG/K for $TmNi_2B_2C$ (Ref. 5) and $ErNi_2B_2C$ (Ref. 6), respectively.

Figure 5(a) shows the low-temperature static volume magnetization M of $DyNi_2B_2C$ for $\mathbf{H}\| c$. From Fig. 2, for this field direction there is only a weak paramagnetic contribution from the Dy sublattice. In Fig. 5(a), the onset of a superconducting magnetization is seen at 6.1 K which becomes nearly independent of T below 4 K. At 2 K the flux expulsion magnetization is 10% of the ideal value of $H/4\pi$ and the shielding fraction is almost 300%. If the crystal is fully superconducting, the latter value indicates a demagnetization factor of 0.66, consistent with that calculated (0.68) for an ellipsoid of revolution with the sample dimensions.

To further confirm that the superconductivity in $DyNi_2B_2C$ is a bulk rather than a surface effect, the $M(T)$ of a powder sample made by crushing a single crystal of $DyNi_2B_2C$ was measured [Fig. 5(b)]. T_N is now seen at ≈ 10.2 K. In addition, a clear onset of a superconducting transition is seen at 5.9 K (see inset). Due to the contribution from the paramagnetic Dy sublattice, the measured magnetization does not become diamagnetic until somewhat lower temperatures. At 2 K the diamagnetic M/H for the field-cooled measurement is 60% of $1/4\pi$ and the zero-field-cooled shielding fraction is 140% which is close to the value (150%) anticipated from the powder average demagnetization factor. The polycrystalline data in Fig. 5(b) and the single-crystal data in Fig. 5(a) show a markedly different temperature dependence of the diamagnetism. For the polycrystalline sample there is an onset of superconductivity at 5.9 K followed by a shallow increase of the diamagnetic magnetization on cooling to 4 K, below which there is a rapid increase of diamagnetism. For the single-crystal sample there is a much more uniform and rapid increase of diamagnetism on cooling below 6.1 K which is nearly complete by 4 K.

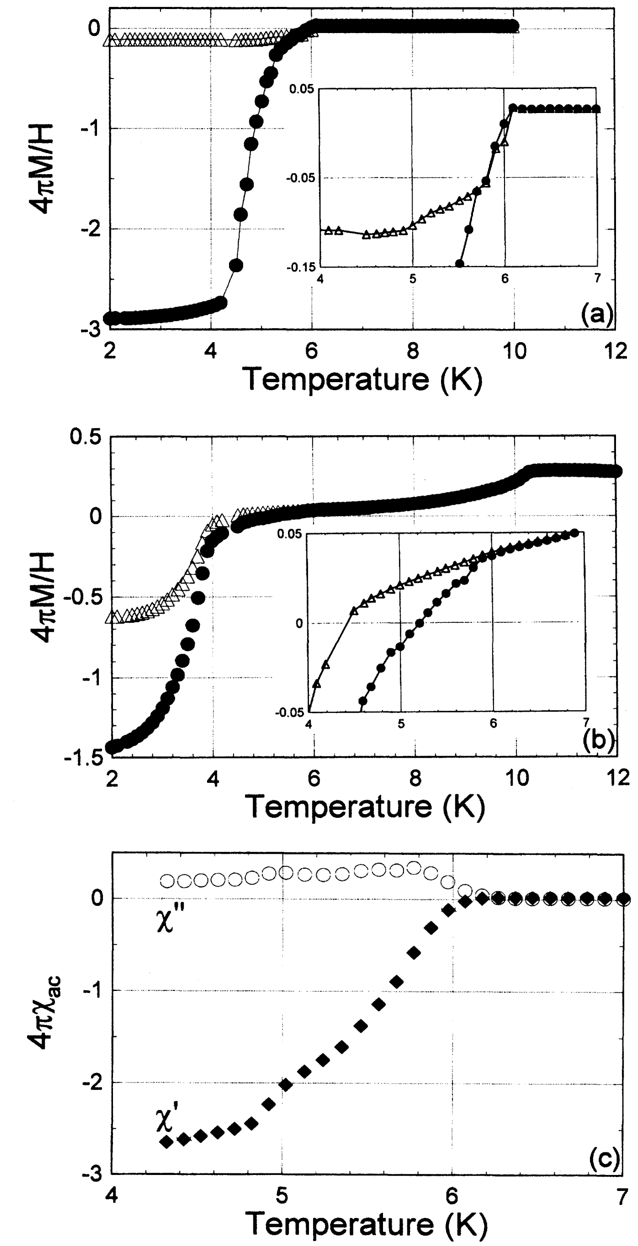

FIG. 5. Temperature-dependent magnetization M of $DyNi_2B_2C$: (a) static M with $\mathbf{H}\|c=10$ G: zero-field-cooled (ZFC) data (circles) and field-cooled/warming (FCW) data (triangles); (b) static M of a powdered single crystal with $H=10$ G: ZFC data (circles) and FCW data (triangles); and (c) real (χ', diamonds) and imaginary (χ'', circles) parts of the ac susceptibility χ_{ac} of the same single crystal used in (a) with $H_{ac}=0.125$ G at a frequency of 125 Hz.

Figure 5(c) shows the ac susceptibility χ_{ac} for $\mathbf{H}_{ac}\|c$ taken on the same single-crystal sample that was used to provide the data shown in Fig. 5(a). The real part of χ_{ac} shows a clear onset of diamagnetism below 6.3 K. In addition, below 6.3 K there is an increase in the imaginary part. Both of these features are consistent with a bulk T_c of 6.3 K.

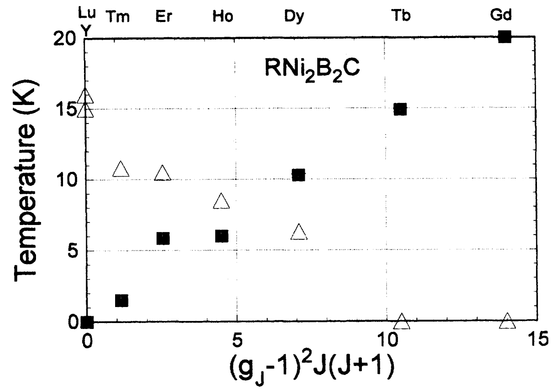

FIG. 6. Néel temperature T_N (squares) and superconducting transition temperature T_c (triangles) vs de Gennes factor $(g_J-1)^2J(J+1)$ for $DyNi_2B_2C$ and other RNi_2B_2C (R=Gd, Tb, Ho, Er, Tm, Lu, and Y) (Refs. 3–7,9,10,14,15,17) single crystals.

Figures 2–5 clearly indicate the existence of a bulk antiferromagnetic transition at $T_N=10.3$ K and a bulk superconducting transition at $T_c=(6.2\pm0.1)$ K in single-crystal $DyNi_2B_2C$. The latter result is in conflict with an earlier report[8] on a polycrystalline sample of $DyNi_2B_2C$ that showed no superconductivity above 2 K. One possible explanation for this difference is that there may be some residual strain in polycrystalline samples leading to an extrinsic suppression of T_c. As shown in Figs. 5(a) and 5(b), a broadening and suppression of the majority of the superconducting transition occurred in our powdered single-crystal sample. Another conspicuous difference between the polycrystalline and single-crystal samples is the value of the residual resistivity ρ_0 at $T>T_c$: for our single-crystal sample $\rho_0(7\text{ K})=2.2\ \mu\Omega$ cm (Fig. 3), while for the polycrystalline sample[8] $\rho_0(7\text{ K})>20\ \mu\Omega$ cm. This difference in ρ_0 may indicate that $DyNi_2B_2C$ shows a variability in composition and/or in the degree of crystallographic ordering; such variabilities could strongly affect T_c as in A-15 compounds such as Nb_3Ge.[16]

With $T_c<T_N$, the question of whether the T_c of $DyNi_2B_2C$ follows de Gennes scaling is a salient one. Figure 6 shows the T_N and T_c values for single crystals of RNi_2B_2C (R= Gd-Tb, Lu, and Y)[3–7,10,11,14,15,17] vs the de Gennes factor $(g_J-1)^2J(J+1)$, where g_J is the Landé factor and J is the total angular momentum of the R^{3+} Hund's rule ground state. Good overall de Gennes scaling is seen for the whole heavy rare-earth series for both T_c and T_N. This indicates that both T_N and the suppression of T_c originate from the same conduction electron-local moment exchange interaction. In particular, our T_c value for single-crystal $DyNi_2B_2C$ is on the order of that expected from the variation of T_c vs de Gennes factor for the other superconducting members.

In summary, temperature-dependent electrical resistivity, static magnetization, and ac susceptibility measurements have revealed the onset of bulk superconductivity in single-crystal $DyNi_2B_2C$ at $T_c=(6.2\pm0.1)$ K, which is significantly lower than the antiferromagnetic ordering (Néel) temperature at $T_N=10.3$ K. $DyNi_2B_2C$ is the first member of the RNi_2B_2C series to exhibit $T_c<T_N$ and also appears to be a

crystallographically ordered compound outside of the heavy-fermion family to show this order of transition temperatures. While there is good overall de Gennes scaling of T_c and T_N across the RNi$_2$B$_2$C series, it is still an open question as to how well de Gennes scaling will work for a series of materials where T_c is lowered through T_N in a more continuous manner. Since $T_c < T_N$ for DyNi$_2$B$_2$C and $T_c > T_N$ for (Ho,Er,Tm)Ni$_2$B$_2$C, a study of the crossover of T_c and T_N in, e.g., $(Ho_{1-x}Dy_x)Ni_2B_2C$ solid solutions should be very interesting.

The authors are grateful to the Ames Laboratory Materials Preparation Center for supplying the high-purity dysprosium metal. Ames Laboratory is operated for the U.S. Department of Energy by Iowa State University under Contract No. W-7405-Eng-82. This work was supported by the Director for Energy Research, Office of Basic Energy Sciences.

[1] For a review of magnetic superconductors as of 1990, see Ø. Fischer, in *Ferromagnetic Materials*, edited by K. H. J. Buschow and E. P. Wohlfarth (North-Holland, Amsterdam, 1990), Vol. 5, p. 465.

[2] R. J. Cava *et al.*, Nature (London) **367**, 252 (1994); T. Siegrist *et al.*, *ibid.* **367**, 254 (1994).

[3] M. Xu *et al.*, Physica C **227**, 321 (1994); M. Xu *et al.*, Physica C **235-240**, 2533 (1995).

[4] R. Movshovich *et al.*, Physica C **227**, 381 (1994).

[5] B. K. Cho, M. Xu, P. C. Canfield, L. L. Miller, and D. C. Johnston, Phys. Rev. B **52**, 3676 (1995).

[6] B. K. Cho, P. C. Canfield, L. L. Miller, D. C. Johnston, W. P. Beyermann, and A. Yatskar, Phys. Rev. B **52**, 3684 (1995).

[7] P. C. Canfield *et al.*, Physica C **230**, 397 (1994).

[8] H. Eisaki *et al.*, Phys. Rev. B **50**, 647 (1994).

[9] A. I. Goldman *et al.*, Phys. Rev. B **50**, 9668 (1994).

[10] J. Zarestky *et al.*, Phys. Rev. B **51**, 678 (1995).

[11] In the case of heavy-fermion superconductors, the moments remaining on the ordering $4f$ sites at low T are greatly reduced through hybridization with the conduction electrons. This class of magnetic superconductors is considered to be fundamentally different from those discussed here.

[12] H. C. Ku, F. Acker, and B. T. Matthias, Phys. Lett. **76A**, 399 (1980); L. D. Woolf *et al.*, J. Low. Temp. Phys. **51**, 117 (1983).

[13] JCPDS-International Center for Diffraction, Powder Data File Card Number 25-576.

[14] P. Dervenagas, J. Zarestky, C. Stassis, A. I. Goldman, P. C. Canfield, and B. K. Cho, Physica B **212**, 1 (1995).

[15] B. K. Cho, P. C. Canfield, and D. C. Johnston (unpublished).

[16] J. R. Gavaler, Appl. Phys. Lett. **23**, 480 (1973); A. R. Sweedler, D. G. Schweitzer, and G. W. Webb, Phys. Rev. Lett. **33**, 168 (1974).

[17] P. C. Canfield, B. K. Cho, and K. W. Dennis, Physica B (to be published).